Dalton Transactions

Cite this: *Dalton Trans.*, 2012, **41**, 1792

www.rsc.org/dalton

PAPER

The synthesis and photophysical studies of cyclometalated Pt(II) complexes with *C*,*N*,*N*-ligands containing imidazolyl donors†

Yu-Man Ho,[a] Chi-Kin Koo,[a] Ka-Leung Wong,[b] Hoi-Kuan Kong,[a] Chris Tsz-Leung Chan,[c] Wai-Ming Kwok,[c] Cheuk-Fai Chow,[a] Michael Hon-Wah Lam*[a] and Wai-Yeung Wong[b]

Received 3rd June 2011, Accepted 4th November 2011
DOI: 10.1039/c1dt11037c

Two new *C*,*N*,*N*-type ligands (HL_2 and HL_3), containing a C_{phenyl}, a $N_{pyridyl}$, and a $N_{imidazolyl}$ donor, and their cycloplatinated complexes, [Pt(L_2)Cl] (**1**), [Pt(L_3)Cl] (**2**), [Pt(L_2)(PPh_3)]$^+$ (**3**) and [Pt(L_3)(PPh_3)]$^+$ (**4**), have been successfully synthesized and characterized. Spectroscopic and ^{3}MLCT luminescent properties of these Pt(II) cyclometalated complexes were found to be pH dependent. This was attributed to the protonation/deprotonation of the acidic 1-imidazolyl-*NH* moieties on the ligands. All the cycloplatinated complexes (both protonated and deprotonated forms) possessed two-photon excitability with two-photon absorption cross-sections ranging from 6.0 to 30.0 GM (protonated forms) and from 16.2 to 24.9 GM (deprotonated forms).

Introduction

Cyclometalation of a d^8 Pt(II) centre by conjugated tridentate phenyl-substituted pyridyl and bipyridyl ligands with low-lying π*-orbitals is a well-established strategy to achieve novel photophysical properties.[1] These cycloplatinated luminophores display long-lived ^{3}MLCT photoluminescence at room temperature and are potentially useful in fields of optoelectronics, chemosensing and bio-labeling.[2] The strong σ-donating deprotonated C-donor of these cyclometalating ligands separates the luminescent MLCT excited states of the organometallic complexes from their ligand-field excited states, which are generally non-emissive at room temperature in solutions.[3] The coordination geometry of these tridentate ligands can also fix the d^8 Pt(II) centre in a square-planar configuration and minimizes radiationless decay due to D_{2d} distortion.[4] The usual approach to fine-tune the photophysical properties of this class of cyclometalated Pt(II) luminophores is *via* the modification of the electronic properties of the cyclometalating and ancillary ligands, commonly through the incorporation of electron-withdrawing and electron-donating substituents.[5] In recent years, another strategy which involves the substitution of one of the pyridyl *N*-donor of the cyclometalating ligands by other 5-membered aromatic *N*-heterocyclic donors has received increasing attention.[5d,6] We have developed a series of π-conjugated cyclometalated ligands with the *C*,*N*,*N* coordination motif composed of a C_{phenyl}, a $N_{pyridyl}$, and a $N_{pyrazolyl}$ donor (HL_1, Fig. 1).[7] The 1-pyrazolyl-*NH* of the 1,2-azole (pyrazole) donors in those ligands are free for further chemical interactions. The room temperature luminescent ^{3}MLCT excited states of their corresponding Pt(II) complexes were found to be accessible *via* two-photon excitation. This, together with their low cytotoxicity, renders them to be useful

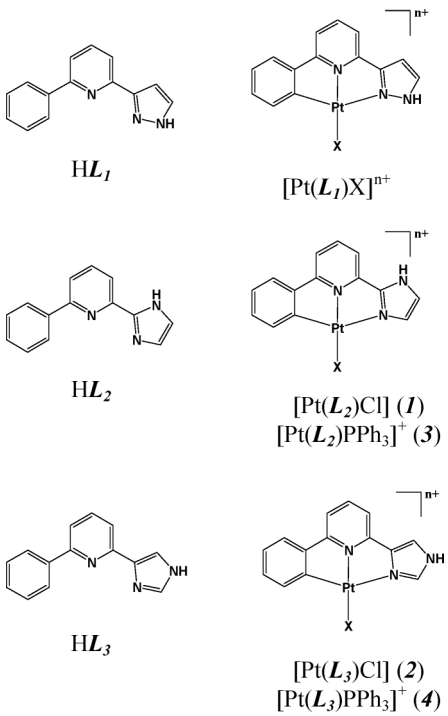

Fig. 1 Chemical structures of the 1,2-/1,3-azole-containing *C*,*N*,*N* ligands and their cycloplatinated complexes.

[a]*Department of Biology & Chemistry, City University of Hong Kong, 83 Tat Chee Avenue, Hong Kong SAR, China. E-mail: bhmhwlam@cityu.edu.hk*
[b]*Department of Chemistry, Hong Kong Baptist University, Waterloo Road, Kowloon Tong, Hong Kong SAR, China*
[c]*Department of Applied Biology & Chemical technology, Hong Kong Polytechnic University, Hung Hom, Hong Kong SAR, China*

† Electronic supplementary information (ESI) available: Additional data. CCDC reference numbers 828775–828777. For ESI and crystallographic data in CIF or other electronic format see DOI: 10.1039/c1dt11037c

two-photon live cell imaging fluorophores.[8] Besides, luminescent properties of this class of new cyclometalated Pt(II) complexes are also pH dependent. The pK_a of [Pt($\boldsymbol{L_1}$)(PPh_3)]$^+$ was found to be *ca.* 4.0.[7c]

These interesting properties of H$\boldsymbol{L_1}$ have prompted us to explore other analogous ligand designs that contain the more basic 1,3-azole donors, H$\boldsymbol{L_2}$ and H$\boldsymbol{L_3}$ (Fig. 1). Spectroscopic, luminescent and photophysical properties of their cyclometalated Pt(II) complexes were studied to comprehend the effects of electronic properties of the imidazolyl ring on these *C*,*N*,*N* coordination motifs.

Experimental

Materials and general procedures

All starting materials, 2,6-dibromopyridine, *n*-butyl lithium (2.5 M in hexane), *N*,*N*-dimethylformamide, *N*,*N*-dimethylacetamide, phenylboronic acid, aqueous glyoxal (40%), aqueous NH_3 (30%), bromine, hydrobromic acid in acetic acid (33%), formamide, triethylamine and K_2PtCl_4 were purchased from commercial sources and used as received unless stated otherwise. Solvents used for synthesis were of analytical grade. Diethyl ether was distilled from sodium-benzophenone and acetonitrile was distilled from anhydrous calcium hydride prior to use. Acetonitrile for photophysical measurements was distilled over potassium permanganate and calcium hydride. 2-Acetyl-6-phenyl-pyridine, 2-carboxyaldehyde-6-phenyl-pyridine and *tetrakis*-(trisphenylphosphine)palladium were prepared according to literature methods.[9,10]

2-(1*H*-Imidazol-2-yl)-6-phenylpyridine (H$\boldsymbol{L_2}$)

To a solution of 40% aqueous glyoxal in cold ethanol, a solution of 2-carboxyaldehyde-6-phenylpyridine (3 g, 16 mmol) in cold ethanol (10 ml) was added and stirred in an ice bath. Cold aqueous NH_3 (30%, 5.5 ml) was added while maintaining the temperature of the entire mixture below 5 °C. Stirring continued in an ice bath for 2 h and the reaction mixture was allowed to warm up gradually to room temperature overnight. The volume was reduced by gentle warming under vacuum. The remaining solution was extracted several times with ethyl acetate. The organic layer was collected, dried over anhydrous magnesium sulfate, concentrated *in vacuo* and recrystallized from ethyl acetate to give the desired product (1.1 g, 31% yield) as a light yellow solid. ESI-MS: 222 (M + 1)$^+$. ^{1}H NMR (400 MHz, $CDCl_3$): δ 8.12–8.10 (d, 1H), 8.04–8.02 (d, 2H), 7.85–7.81 (t, 1H), 7.68–7.66 (d, 1H), 7.49–7.44 (m, 3H), 7.22 (s, 2H). Anal. Calcd for $C_{14}H_{11}N_3$: C, 76.00; H, 5.01; N, 18.99. Found: C, 75.77; H, 5.01; N, 18.62.

2-(Bromoacetyl)-6-phenyl-pyridine

To a mixture of 2-acetyl-6-phenylpyridine (3.00 g, 16 mmol) and hydrobromic acid (10% solution in acetic acid, 10 ml), a solution of bromine (0.82 ml, 16.8 mmol) in acetic acid (3 ml) was added dropwise over an ice bath. The mixture was stirred at 70 °C overnight, basified with saturated aqueous hydrogen bicarbonate and extracted with ethyl acetate. The organic layer was collected, dried over anhydrous magnesium sulfate, concentrated *in vacuo* and the product was purified by a silica column (CH_2Cl_2 : *n*-hexane/1 : 4) to give the desired product as a yellowish oil (2.9 g, 69% yield). ESI-MS: 277 (M + 1)$^+$. ^{1}H NMR (400 MHz, $CDCl_3$): δ 8.09–8.07 (dt, 2H), 8.05–8.02 (dd, 1H), 7.99–7.97 (dd, 1H), 7.95–7.92 (m, 1H), 7.54–7.46 (m, 3H), 4.99 (s, 2H).

2-(1*H*-Imidazol-4-yl)-6-phenylpyridine (H$\boldsymbol{L_3}$)

2-(Bromoacetyl)-6-phenyl-pyridine (2.76 g, 10 mmol) was dissolved in formamide (16 ml, 0.4 mol) and heated at 155 °C overnight. After that, 30 ml of water was added and the solution was extracted three times with chloroform. The organic layer was combined, dried over anhydrous magnesium sulfate and concentrated *in vacuo*. The resulting dark oil was purified by a silica column (ethyl acetate : *n*-hexane = 2 : 1) and recrystallized with ethyl acetate to give the desired product as a yellowish solid (0.57 g, 26% yield). ESI-MS: 222 (M + 1)$^+$. ^{1}H NMR (400 MHz, $CDCl_3$): δ 8.03–8.01 (d, 2H), 7.89 (s, 1H), 7.78–7.74 (t, 1H), 7.67 (s, 1H), 7.66–7.64 (d, 1H), 7.59–7.57 (d, 1H), 7.49–7.42 (m, 3H), 7.00–6.75 (s, 1H). Anal. Calcd for $C_{14}H_{11}N_3$: C, 76.00; H, 5.01; N, 18.99. Found: C, 75.24; H, 4.95; N, 18.68.

[Pt($\boldsymbol{L_2}$)Cl] (1)

A mixture of the free ligand H$\boldsymbol{L_2}$ (0.20 g, 0.9 mmol) and K_2PtCl_4 (0.38 g, 0.9 mmol) in degassed glacial acetic acid (25 ml) was refluxed for 12 h to give a yellow precipitate. The precipitate was collected by filtration and washed with 10 ml of water, methanol and diethyl ether respectively. Crystals suitable for X-ray crystallography was grown by slow evaporation of an acetone/MeOH solution (0.3 g, 76% yield). ESI-MS: 450 (M – 1)$^-$. ^{1}H NMR (400 MHz, $CDCl_3$): δ 8.18–8.14 (dt, 1H), 7.97–7.90 (dd, 1H), 7.79–7.69 (m, 3H), 7.54–7.46 (m, 2H), 7.18(s, 1H), 7.12–7.02 (dt, 1H). Anal. Calcd for $C_{14}H_{10}N_3PtCl{\cdot}H_2O$: C, 35.87; H, 2.58; N, 8.96. Found: C, 36.29; H, 2.56; N, 8.99.

[Pt($\boldsymbol{L_2}$)(PPh_3)](ClO_4) (3·ClO_4)

To an acetonitrile solution (50 ml) of **1** (0.1 g, 0.22 mmol) was added PPh_3 (0.087 g, 0.33 mmol). The mixture was stirred at room temperature for 12 h. A greenish-yellow suspension was obtained and a methanolic solution of $LiClO_4$ (0.23 g, 2.2 mmol) was added. The mixture was stirred at room temperature for another 12 h and the resulting clear yellow solution was filtered and evaporated to a minimum amount. The desired product was precipitated by the addition of diethyl ether as a bright greenish-yellow solid. The product was collected by filtration, washed with diethyl ether and recrystallized by slow vapor diffusion of diethyl ether into an acetonitrile solution (0.12 g, 70% yield). ESI-MS: 677 (M)$^+$. ^{1}H NMR (400 MHz, $CDCl_3$): δ 8.28–8.24 (t, 1H), 8.12–8.10 (d, 1H), 7.89–7.84 (m, 7H), 7.77–7.74 (dd, 1H), 7.69–7.64 (m, 3H), 7.62–7.57 (m, 6H), 7.46–7.46 (d, 1H), 7.07–7.03 (dt, 1H), 6.708–6.667 (dt, 1H), 6.423–6.401 (m, 1H), 4.505–4.501 (s, 1H). Anal. Calcd for $C_{32}H_{25}N_3O_4PPtCl$: C, 49.46; H, 3.24; N, 5.41. Found: C, 49.28; H, 3.22; N, 5.44.

[Pt($\boldsymbol{L_3}$)Cl] (2)

Complex **2** was synthesized using the same method as for complex **1**, except the use of H$\boldsymbol{L_3}$ as the ligand. Yield 71%. ESI-MS: 450 (M – 1)$^-$. ^{1}H NMR (400 MHz, $CDCl_3$): δ 8.43–8.36 (d, 1H), 8.23–7.99 (m, 2H), 7.96–7.88 (dd, 1H), 7.77–7.58 (m, 1H), 7.72–7.70

(dd, 1H), 7.56–7.523 (m, 1H), 7.24–7.21 (m, 1H), 7.13–7.06 (m, 1H). Anal. Calcd for $C_{14}H_{10}N_3PtCl{\cdot}H_2O$: C, 35.87; H, 2.58; N, 8.96. Found: C, 36.39; H, 2.59; N, 8.98.

[Pt(*L*$_3$)(PPh$_3$)](ClO$_4$) (**4**·ClO$_4$)

Complex **4** was synthesized using the same method as for complex **3**. Yield 79%. ESI-MS: 677 $(M)^+$. ^{1}H NMR (400 MHz, $CDCl_3$): δ 8.24–8.20 (m, 2H), 8.03–8.01 (d, 1H), 7.95–7.93 (d, 1H), 7.90–7.85 (m, 6H), 7.77–7.75 (dd, 1H), 7.68–7.64 (m, 3H), 7.62–7.58 (m, 6H), 7.07–7.03 (dt, 1H), 6.70–6.66 (dt, 1H), 6.47–6.44 (m, 1H), 5.01–5.01 (s, 1H). Anal. Calcd for $C_{32}H_{25}N_3O_4PPtCl$: C, 49.33; H, 3.24; N, 5.41. Found: C, 49.28; H, 3.22; N, 5.43.

Physical measurements and instrumentation

Infrared spectra in the range 500–4000 cm^{-1} in KBr plates were recorded on a Perkin Elmer Model FTIR-1600 spectrometer. UV-Vis spectra were measured on a Hewlett Packard 8452A ultraviolet visible diode array spectrophotometer. Emission spectra were recorded using a Horiba FluoroMax-3 spectrofluorimetric with 5 nm slit width and 0.5 s integration time. Acid–base properties of the cycloplatinated complexes were measured in 2 : 1 DMF : aqueous buffer media. Buffer solutions with similar ionic strength, $I = 0.01$, but different pH were prepared according to Perrin and Dempsey.[11] Chloroacetic acid/chloroacetate buffer system was adopted for pH < 3.4, while succinic acid/succinate buffer system was adopted for pH > 3.4. Acid dissociation constants, pK_a, of the cycloplatinated complexes were estimated from the absorbances or luminescent intensities of these complexes at their selected wavelengths of maximum spectral changes in a series of organic aqueous buffer solutions of different pH. The best fitted sigmoid curve (by the non-linear curve fitting algorithm of the Microcal Origin 5.0 software) of the absorbance/luminescent intensity *vs.* pH plot of each complex was used to determine the media pH values where maximum and minimum absorbance/luminescent intensity occurred. The corresponding pK_a of the complex was taken as the mid-pH value between the maximum and minimum pH values. Low-temperature (77 K) emission spectra were collected in 5-mm diameter quartz tubes which were placed in a liquid nitrogen Dewar equipped with quartz windows. ^{1}H NMR spectra were recorded using a Varian YH300 300 MHz NMR spectrometer. Electrospray (ESI) mass spectra were measured by a PE SCIEX API 365 LC/MS/MS system.

Emission quantum yields were measured by the method of Demas and Crosby[12] with $[Ru(bpy)_3](PF_6)_2$ in degassed acetonitrile as the standard ($\phi_r = 0.062$). Lifetime measurements were performed by a nitrogen laser (Spectra Physics) at 337 nm with the maximum power of 15 mW. The luminescence was dispersed by a monochromator and was detected using a cooled R636-10 Hamamastu photon-multiplier (PMT) in combination with a lock-in amplifier system. The decay spectra were monitored by a HP54522A 500 MHz oscilloscope. Sample and standard solutions were degassed with at least three freeze–pump–thaw cycles.

Multi-photon excitation experiments were carried out using a femtosecond mode-locked Ti:Sapphire laser system (output beam ~ 150 fs duration and 1 kHz repetition rate). The 700–900 nm pump wavelengths were generated from a commercial optical parametric amplifier (Coherent) pumped by the SHG of the 800 nm femtosecond pulses. The lasers were focused to a spot size of *ca.* 50 μm *via* a f = 10 cm lens onto the sample. The emitting light was collected with a backscattering configuration into a 0.5 m spectrograph and detected by a liquid nitrogen-cooled CCD detector. A power meter was used to monitor the uniform excitation.

Crystal structure determination†

Crystallographic data for complexes **1**, **3**·ClO$_4$ and **4**·ClO$_4$ are tabulated in the ESI (Table S1).† All intensity data were collected at 293 K on a Bruker Axs SMART 1000 CCD area detector using graphite-monochromated Mo-Kα radiation (λ = 0.71073 Å). All collected frames were processed with the software SAINT[13] and absorption correct was applied (SADABS[14]) to the collected reflections. The structure of the complex was solved by direct methods (SHELXTL[15]) in conjunction with standard difference Fourier syntheses. All non-hydrogen atoms were assigned with anisotropic displacement parameters. The hydrogen atoms were generated in their idealized positions and allowed to ride on the respective carbon atoms.

Results and discussion

Synthesis and characterization

The two new *C*,*N*,*N*$_{imidazolyl}$ ligands, H***L***$_2$ and H***L***$_3$, are structurely related to each other, with the only difference in the orientation of the imidazolyl moiety relative to the central pyridyl ring. H***L***$_2$ involves a 2-(6-phenylpyridyl) substitutent on the imidazole at the C-2 position while H***L***$_3$ has the substitution at the C-4 position. This causes a significant difference in the conjugation of π-electrons over the tridentate ligands. There is an unbranched system of conjugated π-bonds from the central pyridine to the imidazole (head-to-tail type of conjugation) in H***L***$_2$, but not for H***L***$_3$.[16] Theoretical studies on analogous systems of 2- and 4-phenylimidazole have revealed that due to the relatively longer conjugate chain of π-electrons, 2-phenylimidazole showed a higher interaction energy between the phenyl and the heterocyclic rings, and a lower π–π* energy gap, than 4-phenylimidazole.[17] Such differences in electronic properties are also expected in H***L***$_2$ and H***L***$_3$.

These new *C*,*N*,*N*-ligands were prepared by modified literature procedures outlined in Scheme 1. 2-Bromo-6-carboxyaldehyde-pyridine and 2-acetyl-6-bromopyridine were obtained from 2,6-dibromopyridine, *via* lithiation with *n*-butyl lithium and *N*,*N*-dimethylformamide or *N*,*N*-dimethylacetamide as substrate respectively. They were then converted to 2-carboxyaldehyde-6-phenylpyridine and 2-acetyl-6-phenylpyridine, respectively, by palladium catalyzed Suzuki cross-coupling reaction with phenylboronic acid. By treating 2-carboxyaldehyde-6-phenylpyridine with 40% aqueous glyoxal and 30% aqueous ammonia, pure H***L***$_2$ was obtained after recrystallization with ethyl acetate. The intermediate of H***L***$_3$ was obtained by treating 2-acetyl-6-phenylpyridine with bromine in acetic acid. The resulting 2-(bromoacetyl)-6-phenyl-pyridine was refluxed with formamide and H***L***$_3$ was obtained after purification with column chromatography and recrystallization.

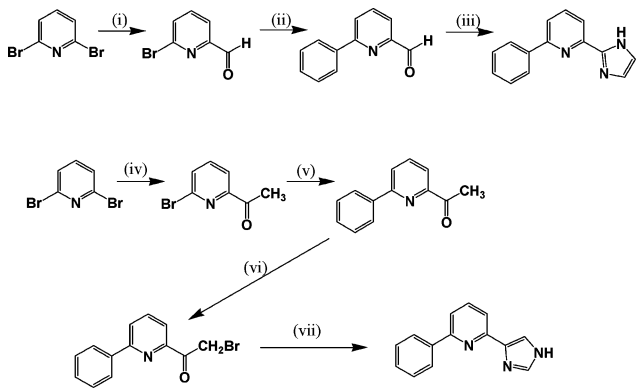

Scheme 1 Synthesis of the new *C*,*N*,*N*-ligands: (i) *n*-BuLi, *N*,*N*-dimethylformamide, Et_2O, –60 °C; (ii) phenylboronic acid in toluene, $Pd(PPh_3)_4$ (5 mol%), K_2CO_3 in H_2O, reflux; (iii) 40% aqueous glyoxal, 30% NH_3, EtOH, 0 °C; (iv) *n*-BuLi, *N*,*N*-dimethylacetamide, Et_2O, –60 °C; (v) phenylboronic acid in toluene, $Pd(PPh_3)_4$ (5 mol%), K_2CO_3 in H_2O, reflux; (vi) Br_2, HBr in acetic acid, 70 °C; (vii) formamide, 155 °C.

The neutral cycloplatinated complexes, [Pt(***L*****$_2$**)Cl] (**1**) and [Pt(***L*****$_3$**)Cl] (**2**), were obtained in *ca.* 70% yield by refluxing the corresponding ligands with K_2PtCl_4 in glacial acetic acid for 12 h.[18] Substitution of the chloride ligand by triphenylphosphine in acetonitrile generated the cationic cycloplatinated complexes $[Pt(\boldsymbol{L}_2)(PPh_3)]^+$ (**3**) and $[Pt(\boldsymbol{L}_3)(PPh_3)]^+$ (**4**). All these Pt(II) $C,N,N_{imidazoyl}$ cyclometalated complexes were characterized by ^{1}H NMR, mass spectrometry and elementary analysis. Structures of complexes **1**, **3**·ClO_4 and **4**·ClO_4 were revealed by X-ray crystallography.

Crystal structures

X-Ray quality single crystals of **1** were grown by slow evaporation of its acetone/methanol solution, and those of **3**·ClO_4 and **4**·ClO_4 were grown by slow diffusion of diethyl ether into their acetonitrile solutions. Fig. 2 shows the perspective view and crystal packing of **1**. Selected bond lengths and angles are listed in Table 1. The coordinate geometry of the Pt centre is a distorted square planar configuration with a C(1)–Pt(1)–N(2) angle of 160.8(2)°. Bond distances of Pt(1)–C(1), Pt(1)–N(1) and Pt(1)–N(2) are 1.990(5), 1.953(4) and 2.114(5) Å respectively, which are all comparable to the analogous [Pt(***L*****$_1$**)Cl].[7b] The crystal lattice of **1** contains two planar [Pt(***L*****$_2$**)Cl] units that are stacked in a head-to-tail fashion with a Pt–Pt distance of 4.89 Å and parallel to each other. No intermolecular Pt–Pt interaction is evident. On the other hand, the interplanar separation was measured to be 3.848 Å indicating the presence of weak π–π interaction between the ligands of the two [Pt(***L*****$_2$**)Cl] units. Continuous chains with alternating long and short Pt–Pt distances of 4.89 Å and 6.437 Å resulted from the packing of these dimeric units.

Table 1 Selected bond lengths (Å) and angles (°) of complex **1**

Pt(1)–C(1)	1.990(5)	Pt(1)–N(1)	1.953(4)
Pt(1)–N(2)	2.114(5)	Pt(1)–Cl(1)	2.3129(14)
C(1)–Pt(1)–N(1)	81.09(19)	C(1)–Pt(1)–Cl(1)	98.07(16)
N(1)–Pt(1)–N(2)	79.79(16)	N(2)–Pt(1)–Cl(1)	101.06(12)
N(1)–Pt(1)–Cl(1)	179.09(12)	C(1)–Pt(1)–N(2)	160.8(2)

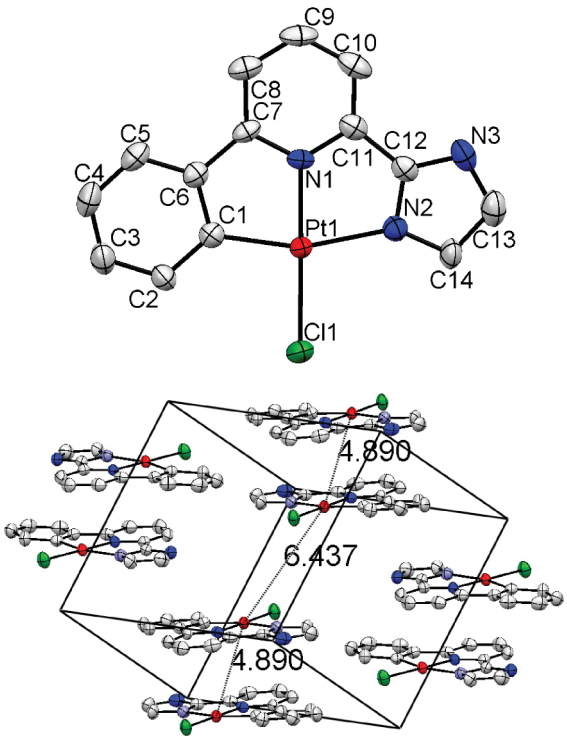

Fig. 2 Molecular structure and crystal packing mode of [Pt(***L*****$_2$**)Cl] (**1**) with the numbering scheme adopted. Thermal ellipsoids are shown at the 50% probability level.

Table 2 Selected bond lengths (Å) and angles (°) of complex **3**·ClO_4

Pt(1)–C(1)	2.019(3)	Pt(1)–N(1)	2.022(2)
Pt(1)–N(2)	2.124(2)	Pt(1)–P(1)	2.2426(6)
C(1)–Pt(1)–N(1)	80.64(10)	C(1)–Pt(1)–P(1)	97.94(8)
N(1)–Pt(1)–N(2)	78.21(9)	N(2)–Pt(1)–P(1)	103.26(6)
N(1)–Pt(1)–P(1)	177.56(6)	C(1)–Pt(1)–N(2)	158.77(10)

Fig. 3 shows the perspective view and crystal packing of the cationic complex **3**. Selected bond lengths and angles are listed in Table 2. Similar to the analogous $[Pt(\boldsymbol{L}_1)(PPh_3)]^+$, **3** has a slightly distorted square planar configuration. It has a C(1)–Pt(1)–N(2) angle of 158.77(10)° and a Pt(1)–P(1) bond length of 2.2426(6) Å, both comparable to that of $[Pt(\boldsymbol{L}_1)(PPh_3)]^+$. No Pt–Pt interaction is observed among platinum centres in the crystal packing and the shortest Pt–Pt distance measured is 6.420(5) Å. This is probably due to the presence of the bulky PPh_3 ligand which hinders the approach of the two Pt(II) centres. The two $[Pt(\boldsymbol{L}_2)(PPh_3)]^+$ units are paired in a head-to-tail fashion with an interplanar separation between the $C,N,N_{imidazolyl}$ ligands of 3.630 Å indicating the presence of weak π–π interactions. The phenylpyridyl part of the ligand is mainly involved in the stacking.

While no X-ray quality crystal of the neutral [Pt(***L*****$_3$**)Cl] (**2**) could be successfully grown, its conversion into cationic $[Pt(\boldsymbol{L}_3)(PPh_3)]^+$ (**4**) *via* the substitution of the chloride ancillary ligand by a neutral triphenylphosphine afforded X-ray quality crystals that enabled the crystallographic characterization of the ligand ***L*****$_3$** with its special orientation of the imidazole-ring. Fig. 4 shows the perspective view and crystal packing of the cationic complex **4**, with selected bond lengths and angles listed in Table 3. Closely resembling **3**, complex **4** has a slightly distorted square planar

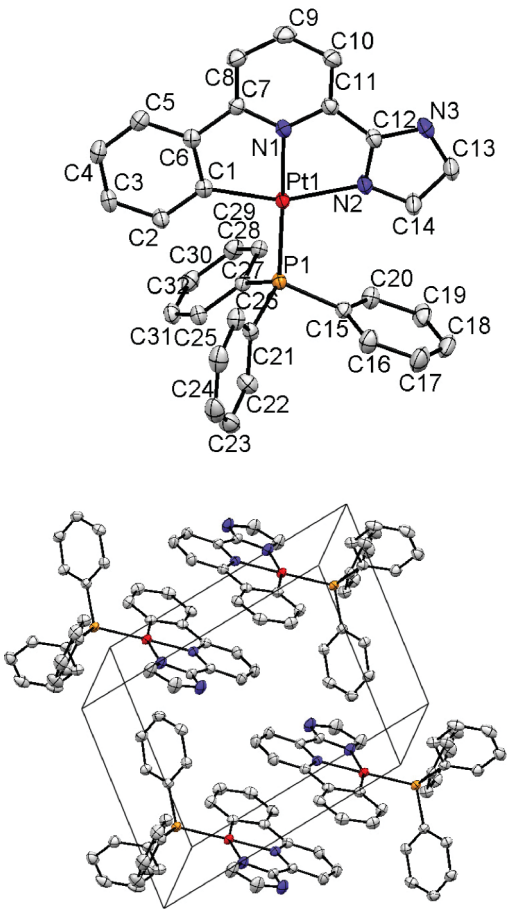

Fig. 3 Molecular structure and crystal packing mode of $[Pt(\boldsymbol{L}_2)(PPh_3)]^+$ (**3**) with the numbering scheme adopted. Thermal ellipsoids are shown at the 50% probability level.

Table 3 Selected bond lengths (Å) and angles (°) of complex **4**·ClO_4

Pt(1)–C(1)	2.005(4)	Pt(1)–N(1)	2.025(3)
Pt(1)–N(2)	2.107(3)	Pt(1)–P(1)	2.2272(9)
C(1)–Pt(1)–N(1)	81.11(15)	C(1)–Pt(1)–P(1)	97.59(11)
N(1)–Pt(1)–N(2)	78.56(14)	N(2)–Pt(1)–P(1)	103.02(9)
N(1)–Pt(1)–P(1)	175.78(9)	C(1)–Pt(1)–N(2)	159.13(15)

configuration. The C(1)–Pt(1)–N(2) angle is 159.13(15)° and the Pt(1)–P(1) bond length is 2.2272(9) Å. No Pt–Pt interaction is observed in the crystal packing of **4** (shortest Pt–Pt distance measured is 6.993 (3)). Two cyclometalated complex units were stacked in a head-to-tail configuration. However, unlike **3**, π–π stacking was observed not between the phenylpyridyl part of the ligand, but between the pyridylimidazolyl part. The distance between the two stacking rings was found to be 3.732 Å. This may be accounted by the observed partial overlapping between imidazole rings of neighbouring stacking unit, with a separation of 3.805 Å.

Spectroscopic and luminescent properties

Detailed spectroscopic and luminescent properties of the new cyclometalated platinum(II) complexes are summerized in the ESI (Table S2)† (where spectroscopic and luminescent data of the previously reported analogous $[Pt(\boldsymbol{L}_1)Cl]$ are also tabulated for

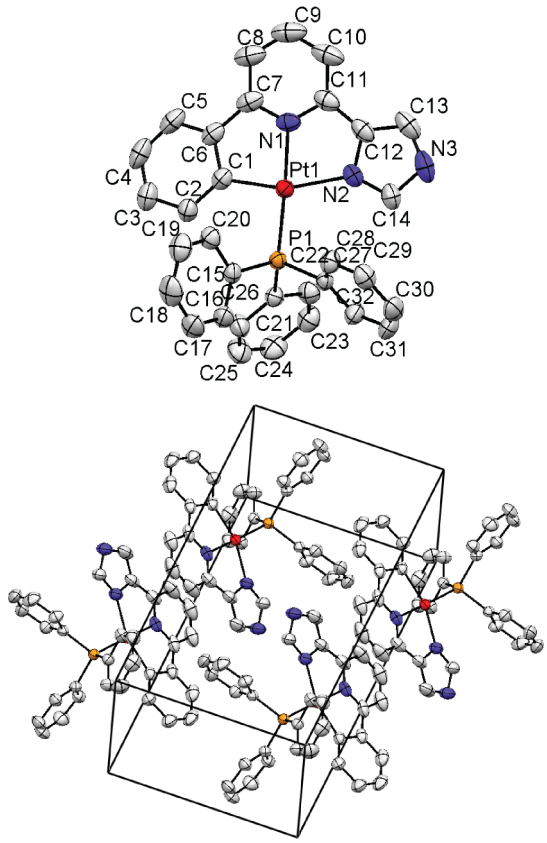

Fig. 4 Molecular structure and crystal packing mode of $[Pt(\boldsymbol{L}_3)(PPh_3)]^+$ (**4**) with the numbering scheme adopted. Thermal ellipsoids are shown at the 50% probability level.

reference). Both the neutral cycloplatinated complexes **1** and **2** display intensive absorption bands at *ca.* 240–375 nm with extinction coefficients (ε) of the order of 10^4 dm^3 mol^{-1} cm^{-1} and a less intense band at *ca.* 375–410 nm with ε of the order of 10^3 dm^3 mol^{-1} cm^{-1} (Fig. 5). By comparing with $[Pt(\boldsymbol{L}_1)Cl]$, those higher energy absorption bands are attributed to the intraligand ($\pi(L) \rightarrow \pi^*(L)$) transitions, while the lower energy absorption bands are assigned the spin-allowed singlet metal-to-ligand charge-transfer (^{1}MLCT) transition. The solvent dependency of transition energy of this absorption band (λ_{max} shifts from 376–400 nm in acetonitrile to 385–413 nm in dichloromethane) supports this assignment. Both complexes show an absorption tail at 410–475 nm that are attributable to the spin-forbidden ^{3}MLCT transition.

For the cationic complexes **3** and **4**, their intraligand transition bands, as well as their ^{1}MLCT and ^{3}MLCT transitions were all blue-shifted *ca.* 40 nm compared to their precursor complexes **1** and **2**.

All four new cycloplatinated complexes show intense photoluminescence in solutions at room temperature. Fig. 6 shows the normalized room temperature excitation and emission spectra of the neutral complexes **1** and **2** in acetonitrile. Complex **1** gives a poorly-resolved emission profile with λ_{max} at 521 nm (τ_o = 1.28 μs; ϕ = 0.18), while complex **2** shows its emission maxima at 503 nm (τ_o = 2.36 μs; ϕ = 0.10), with a well-resolved vibronic structured emission profile at 490–580 nm with spacing of *ca.* 1300 cm^{-1} which correlates to the skeletal vibrational frequency of the $C,N,N_{imidazolyl}$ ligand (Fig. 6). The observed large Stokes shifts and relatively long

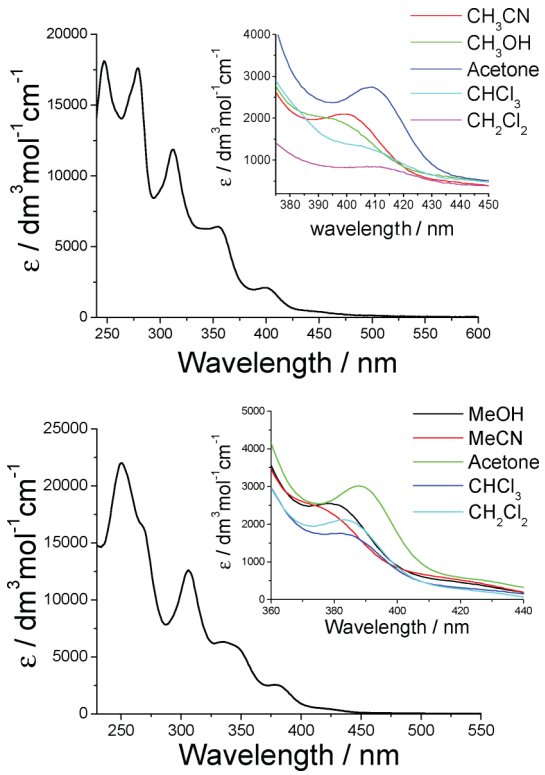

Fig. 5 Spectroscopic properties of [Pt($\boldsymbol{L}_2$)Cl] (**1**) (upper) and [Pt($\boldsymbol{L}_3$)Cl] (**2**) (lower) in acetonitrile at 298 K, with solvent dependence of the absorption band at 375–420 nm shown in the insets.

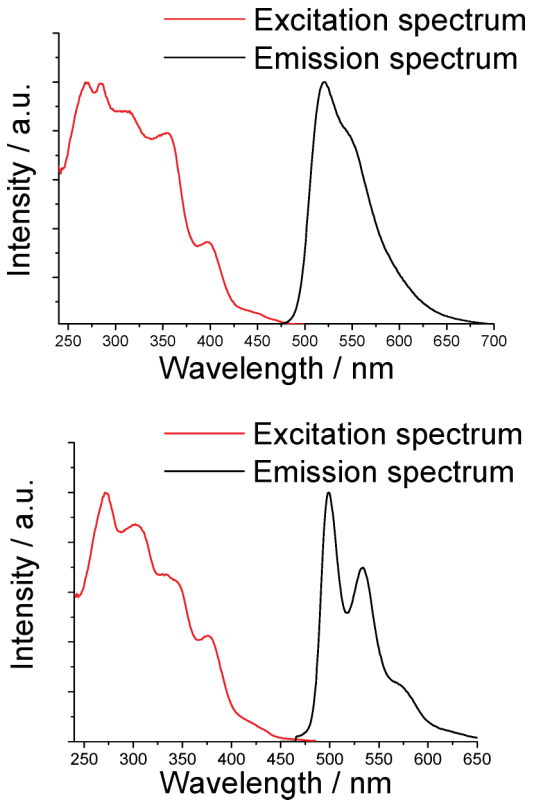

Fig. 6 Normalized excitation and emission spectra of **1** (upper) and **2** (lower) in acetonitrile at room temperature (concentration = 5×10^{-5} M).

emission lifetimes of both complexes suggest that their emissions originate from a spin-forbidden triplet excited state. With reference to [Pt($\boldsymbol{L}_1$)Cl], the luminescence of **1** and **2** can be assigned the ^{3}MLCT transition.

It is interesting to compare the spectroscopic and luminescent properties of both cyclometalated Pt(II) complexes **1** and **2** with 1,3-azole donors in their cyclometalating ligands to those of [Pt($\boldsymbol{L}_1$)Cl] that contains a 1,2-azole (pyrazolyl) donor. Both the electronic and excited-state MLCT transitions of **1** are red-shifted compared to those of [Pt($\boldsymbol{L}_1$)Cl]. Although imidazole is more basic than pyrazole, numerous studies have shown that the imidazolyl-*N* is only slightly stronger in terms of σ-donor strength.[19] On the other hand, imidazole is a relatively poorer π-acceptor than pyrazole.[20] This causes **1** to possess relatively higher energy dπ(Pt) orbitals and a smaller MLCT energy gap compared to [Pt($\boldsymbol{L}_1$)Cl]. Contrary to **1**, energies of both the electronic and excited-state MLCT transitions of complex **2** are higher than those of [Pt($\boldsymbol{L}_1$)Cl]. This is attributable to the cross-conjugate system of $\boldsymbol{L}_3$ resulting in a relatively shorter π-conjugate chain and a higher energy π*(**L**).

Acid–base responses of the spectroscopic and luminescent properties of 3 and 4

The cationic **3** and **4** possess better aqueous solubility than their neutral precursors. They were used to investigate the acid–base properties of the 1-imidazolyl-*NH* functionality on the $\boldsymbol{L}_2$ and $\boldsymbol{L}_3$ in aqueous organic media *via* pH titrations in 2 : 1 DMF : aqueous buffer (with complex concentration of 5×10^{-5} M). Integrity of the cycloplatinated complexes in DMF was checked by ESI-MS in 2 : 1 DMF : acetonitrile. No displacement of the triphenylphosphine ancillary ligand nor the coordinated cyclometalating ligands by DMF was observed (Fig. S1, ESI†). Spectroscopic and luminescent properties of **3** and **4** vary with media pH (Fig. 7 and 8). These phenomena are attributable to the protonation/deprotonation of the 1-imidazolyl-*NH* moiety on $\boldsymbol{L}_2$ and $\boldsymbol{L}_3$. ^{1}H NMR titration of *d*-DMSO solutions of complexes **3** and **4** by triethylamine revealed the disappearance of their 1-imidazolyl-*NH* bands at *ca.* 13.3–14.3 ppm (Fig. S2 and S3, ESI†). A gradual increase of media pH from 3.5 onward results in a continuous red-shift of the intraligand and ^{1}MLCT absorption bands with a series of well defined isosbestic points, indicating a clean conversion between the protonated and deprotonated forms of **3** and **4**. The λ_{max} of the ^{3}MLCT emissions of **3** and **4** at pH < 3.6 are observed at 510 and 491 nm respectively. Their luminescent intensities are reduced, concomitant with slightly red-shifts in λ_{max} to 516 and 498 nm respectively, upon further increase in media pH.

These spectroscopic and luminescent responses of **3** and **4** are similar to other coordination systems in the literature that display spectroscopic or electrochemical pH responses due to the protonation/deprotonation of the imidazolyl functionality.[21] The red-shift of the ^{1}MLCT bands may be the result of a decrease in the bond distance between the anionic deprotonated imidazolyl ligand and the Pt(II) centre that destablizes the d-orbitals and reduces the MLCT gap.[20a]

The pK_a values of **3** and **4** at room temperature are estimated from their spectroscopic responses at selected wavelengths (336 nm in complex **3** and 345 nm in complex **4**) (insets of Fig. 7(a) and 8(a)). They are found to be *ca.* 4.33 (for complex **3**) and 5.08

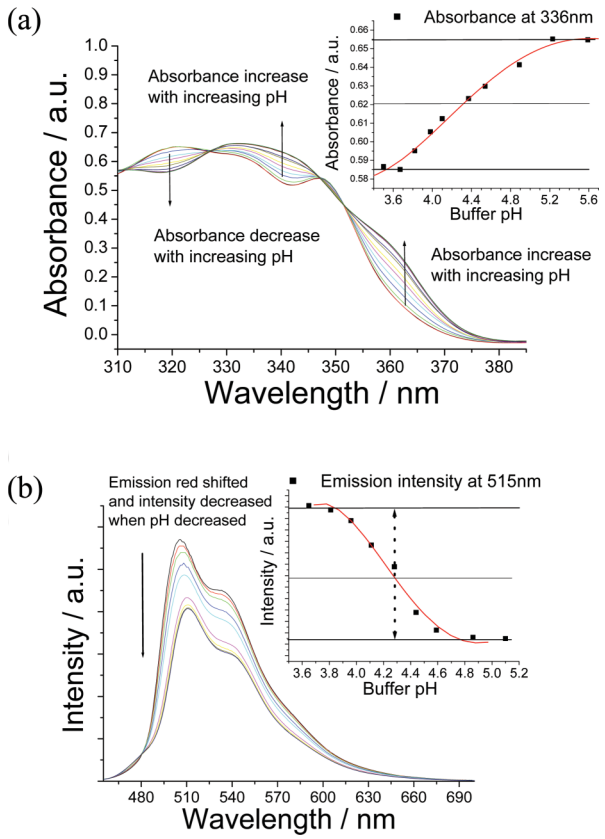

Fig. 7 Spectroscopic (a) and luminescent (b) responses of **3**·ClO_4 in 2 : 1 (v/v) DMF : aqueous buffer (5×10^{-5} M) to changes in media pH at 298 K. (Excitation $\lambda = 345$ nm.)

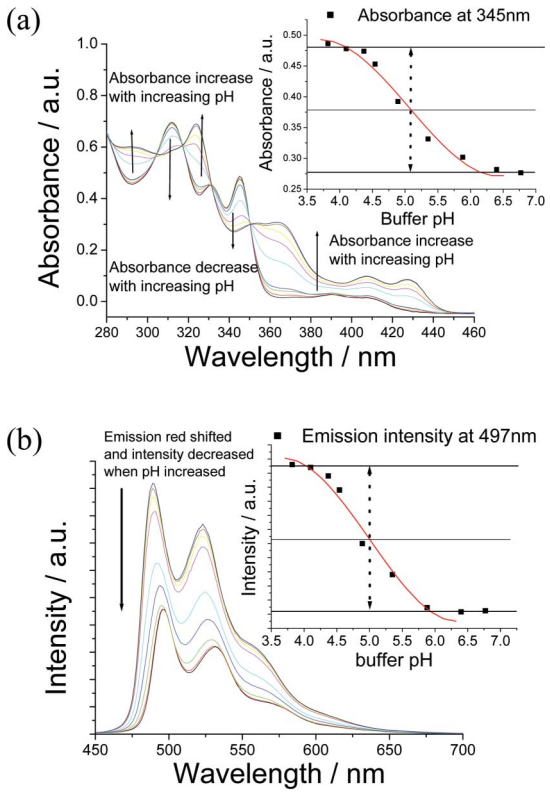

Fig. 8 Spectroscopic (a) and luminescent (b) responses of **4**·ClO_4 in 2 : 1 (v/v) DMF : aqueous buffer (5×10^{-5} M) to changes in media pH at 298 K. (Excitation $\lambda = 345$ nm.)

(for complex **4**), which are considerably higher than that of our previously reported $[Pt(\boldsymbol{L}_1)(PPh_3)]^+$ ($pK_a = 4.0$). This is probably due to the presence of the more basic imidazolyl donors.

Changes in the luminescent properties of **3** and **4** with media pH also enable the estimation of their excited state pK_a* values. From the insets of Fig. 7(b) and 8(b), the pK_a* values of the two complexes are found to be 4.26 (complex **3**) and 5.00 (complex **4**). Such small differences between ground state and excited state acid dissociation constants suggest that the electron promoted to the ligand π*-orbital in the MLCT excited-states of **3** and **4** may not be distributed on the imidazolyl ring of the ligands $\boldsymbol{L}_2$ and $\boldsymbol{L}_3$, where the deprotonation process takes place.[22] Similar observations were also obtained by Deverlay *et al.*[6b] in their asymmetric *N*,*C*,*N* cyclometalated Pt(II) systems that contained *N*-linked 1-arylpyrazoles where the LUMOs were located largely on the six-membered aromatic rings rather than the *N*-heterocycles. Of course, these are just preliminary assessments which have to be further substantiated by time-resolved photophysical measurements. Work towards the further understanding of the excited state photophysics of these cycloplatinated complexes are in progress.

Two-photon induced photophysical properties

Fig. 9 shows the two-photon induced emission spectra and emission-laser power relationship of complexes **1–4** in DMF (concentration = 1×10^{-4} M) by near-IR ($\lambda_{excitation} = 750$ nm) femto-second excitation. These NIR induced emission spectra closely resembles the single-photon ^{3}MLCT emission spectra of

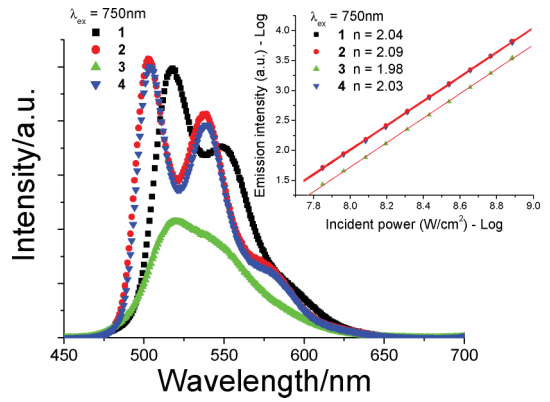

Fig. 9 Two-photon induced luminescent spectra of **1–4** in DMF (concentration = 1×10^{-4} M) at 298 K ($\lambda_{ex} = 750$ nm). The log–log plots of the power dependence of luminescent intensities of the complexes shown in the inset confirm the two-photon excitation processes.

these complexes. The ^{3}MLCT emission induced by two-photon absorption processes were confirmed by the evolution of the intensities of the peak that are plotted as a function of the incident power at 750 nm. The slopes of the log–log plots (1.98–2.09, λ_{ex} = 750 nm) for the cyclometalated Pt(II) complexes confirm the non-linear absorption processes at 750 nm.

The efficiency of the two-photon processes was evaluated by two-photon absorption cross-section measurements with Rhodamine 6G in DMF as the reference standard.[23] All four complexes (**1–4**) possess modest two-photon absorption cross-sections ranging from 6 to 30 GM (GM = 10^{-50} cm^4 s $photon^{-1}$

Table 4 The two-photon absorption cross-section (GM) of complexes **1–4** in neutral, protonated and deprotonated forms

Complex	Neutral[a]	Deprotonated[b,c]
1	12	22.9 (0.025)
2	9	24.9 (0.058)
3	30	16.2 (0.012)
4	6	23.2 (0.009)

[a] Measured in DMF (concentration = 1×10^{-4} M). [b] Measured in DMF with 5% triethylamine. [c] Emission (single-proton) quantum yield are shown in blanket.

molecule^{-1}) (Table 4). To examine whether the deprotonated form of these cycloplatinated luminophores also possess multi-photon excitation and emission properties, we have also measured the two-photon absorption cross-section of the four cycloplatinated complexes in their deprotonated states in DMF (concentration = 1×10^{-4} M) (Table 4 and Fig. S4, ESI†). These deprotonated luminophores also possess modest two-photon absorption cross-section ranging from 16.2 to 24.9 GM.

Conclusions

To conclude, we have developed two new *C*,*N*,*N*-type ligands that contain the more basic imidazolyl donors for the cyclometalation of d^8 Pt(II) centres. The two structural related ligands, HL_2 and HL_3, possess different electronic properties because of the difference in the substitution position of the phenylpyridyl moiety on the imidazole. All the resultant cycloplatinated complexes, [Pt(L_2)Cl] (**1**) and [Pt(L_3)Cl] (**2**), as well as their cationic derviatives, [Pt(L_2)(PPh$_3$)]$^+$ (**3**) and [Pt(L_3)(PPh$_3$)]$^+$ (**4**), are luminescent at room temperature in solutions. The acid–base properties of the 1-imidazolyl-*NH* functionality on both L_2 and L_3 are able to bring about spectroscopic and luminescent responses in the cycloplatinated luminophores. The measured ground state and excited state pK_a values are 4.33 and 4.26, respectively, for Pt(L_2)(PPh$_3$)]$^+$ (**3**), and 5.08 and 5.00, respectively, for [Pt(L_3)(PPh$_3$)]$^+$ (**4**). These pK_a values, especially that of **4**, are physiological relevant. While normal cytoplasmic pH of live cells is in the range of 7.0–7.5, pH in selected intracellular organelles of the endosomal and secretory compartments is much lower due to the action of vacuolar-type proton pumps.[24] For example, pH of lysosomes can be as low as 4.7–4.8.[25] The specific pH luminescent responses of **3** and **4** can be further explored to bring about "switch-on" luminescent imaging of these more acidic organelles in live cells.

All the new cyclometalated platinum(II) complexes are capable of producing two-photon excited ^{3}MLCT emissions from femto-second near-IR ($\lambda_{excitation}$ = 750 nm) two-photon excitation with modest two-photon absorption cross-sections for imaging purposes. This two-photon excitability, combined with their pH luminescent responses, make complexes **3** and **4** potentially useful luminophores for bio-labeling and live-cell imaging.

Acknowledgements

This work is jointly funded by a CERG grant (CityU 101208) from the Research Grant Council and the Areas of Excellence Scheme (AoE/P-03/08) of the University Grants Committee of Hong Kong SAR, China.

Notes and references

1 (*a*) D. Sandrini, M. Masestri, V. Balzani, L. Chassot and A. von Zelewsky, *J. Am. Chem. Soc.*, 1987, **109**, 7720–7724; (*b*) T.-C. Cheung, K.-K. Cheung, S.-M. Peng and C.-M. Che, *J. Chem. Soc., Dalton Trans.*, 1996, 1645–1651; (*c*) J. H. K. Yip and J. J. Vittal, *Inorg. Chem.*, 2000, **39**, 3537–3543; (*d*) H. Yersin and D. Donges, *Top. Curr. Chem.*, **214**, 81–186; (*e*) W. Lu, M. C. W. Chan, K.-K. Cheung and C.-M. Che, *Organometallics*, 2001, **20**, 2477–2486.
2 (*a*) W. Lu, B.-X. Mi, M. C. W. Chan, Z. Hui, C.-M. Che and S.-T. Lee, *J. Am. Chem. Soc.*, 2004, **126**, 4958–4971; (*b*) P. K.-M. Siu, D.-L. Ma and C.-M. Che, *Chem. Commun*, 2005, 1025–1027; (*c*) S. C. F. Kui, S. S.-Y. Chui, C.-M. Che and N. Zhu, *J. Am. Chem. Soc.*, 2006, **128**, 8297–8309; (*d*) J. A. G. Williams, S. Develay, D. L. Rochester and L. Murphy, *Coord. Chem. Rev.*, 2008, **252**, 2596–2611; (*e*) S. W. Botchway, M. Charnley, J. W. Haycock, A. W. Parker, D. L. Rochester, J. A. Weinstein and J. A. G. Williams, *Proc. Natl. Acad. Sci. U. S. A.*, 2008, **105**, 16071–16076; (*f*) C.-M. Che, H.-F. Xiang, S. S.-Y. Chui, Z.-X. Xu, V. A. L. Roy, J. J. Yan, W.-F. Fu, P. T. Lai and I. D. Williams, *Chem.–Asian J.*, 2008, **3**, 1092–1103; (*g*) P. Wu, L.-M. Wong, D.-L. Ma, G. S.-M. Tong, K.-M. Ng and C.-M. Che, *Chem.–Eur. J.*, 2009, **15**, 3652–3656; (*h*) Q. Zhao, F. Li and C. Huang, *Chem. Soc. Rev.*, 2010, **39**, 3007–3030.
3 (*a*) V. M. Miskowski, V. H. Houlding, C.-M. Che and Y. Wang, *Inorg. Chem.*, 1993, **32**, 2518–2524; (*b*) S.-W. Lai and C.-M. Che, *Top. Curr. Chem*, 2004, **241**, 27–63.
4 L. J. Andrews, *J. Phys. Chem.*, 1979, **83**, 3203–3209.
5 (*a*) F. Neve Crispini and S. Campagna, *Inorg. Chem.*, 1997, **36**, 6150–6151; (*b*) S.-W. Lai, M. C. W. Chan, K.-K. Cheung and C.-M. Che, *Organometallics*, 1999, **18**, 3327–3336; (*c*) W. Sun, Z.-X. Wu, Q.-Z. Yang, L.-Z. Wu and C.-H. Tung, *Appl. Phys. Lett.*, 2003, **82**, 850–852; (*d*) W. Lu, B.-X. Mi, M. C. W. Chan, Z. Hui, C.-M. Che, N. Zhu and S.-T. Lee, *J. Am. Chem. Soc.*, 2004, **126**, 4958–4971; (*e*) W. Sun, H. Zhu and P. M. Barron, *Chem. Mater*, 2006, **18**, 2602–2610.
6 (*a*) J. Forniés, V Sicilia, C. Larraz, J. A. Camerano, A. Martin, J. M. Casas and A. C. Tsipis, *Organometallics*, 2010, **29**, 396–1405; (*b*) S. Develay, O. Blackburn, A. L. Thompson and J. A. G. Williams, *Inorg. Chem*, 2008, **47**, 11129–11142.
7 (*a*) C.-K. Koo, B. Lam, S.-K. Leung, M. H.-W. Lam and W.-Y. Wong, *J. Am. Chem. Soc*, 2006, **128**, 16434–16435; (*b*) C.-K. Koo, Y.-M. Ho, C.-F. Chow, M. H.-W. Lam, T.-C. Lau and W.-Y. Wong, *Inorg. Chem*, 2007, **46**, 3603–3612; (*c*) C.-K. Koo, K.-L. Wong, C. W.-Y. Man, H.-L. Tam, S.-W. Tsao, K.-W. Cheah and M. H.-W. Lam, *Inorg. Chem*, 2009, **48**, 7501–7503.
8 C.-K. Koo, L. K.-Y. So, K.-L. Wong, Y.-M. Ho, Y.-W. Lam, M. H.-W. Lam, K.-W. Cheah, C. C.-W. Cheng and W.-M. Kwok, *Chem. Eur. J*, 2010, **16**, 3942–3950.
9 D. Lötscher, S. Rupprecht, H. Stoeckli-Evans and A. Zelewsky, *Tetrahedron: Asymmetry*, 2000, **11**, 4341–4357.
10 D. R. Coulson, *Inorg. Synth.*, 1990, **28**, 107.
11 D. D. Perrin, B. Dempsey, *Buffers for pH and metal ion control*, Chapman and Hall, London, 1974.
12 J. N. Demas and G. A. Crosby, *J. Phys. Chem.*, 1971, **75**, 991.
13 *SAINT Reference Manual*, Siemens Energy and Automation, Madison, WI, 1994–1996.
14 G. M. Sheldrick, *SADABS, Empirical Absorption Correction Program*, University of Göttingen, Germany, 1997.
15 G. M. Sheldrick, *SHELXTL™ Reference Manual, version 5.1*, Siemens, Madison, WI, 1997.
16 (*a*) W. J. Eilbeck, F. Holmes, G. G. Phillips and A. E. Underhill, *J. Chem,. Soc. (A)*, 1967, 1161–1166; (*b*) W. J. Eilbeck and F. Holmes, *J. Chem,. Soc. (A)*, 1967, 1777–1782.
17 V. I. Minkin, S. F. Pozharskii, Y. A. Ostroumov, In *Chemistry of Heterocyclic Compounds*, Vol. 2, pp. 413–420.
18 D. J. Cardenas, A. M. Echavarren and M. C. Ramirez de Arellano, *Organometallics*, 1999, **18**, 3337–3341.
19 (*a*) D. W. Randall, S. D. George, B. Hedman, K. O. Hodgson, K. Fujisawa and E. I. Solomon, *J. Am. Chem. Soc*, 2000, **122**,

11620–11631; (*b*) C. Hu, B. C. Noll, C. E. Schulz and W. R. Scheidt, *Inorg. Chem*, 2010, **49**, 10984–10991.
20 (*a*) P. V. Schatnev, M. S. Shvartsberg, I. Y. Bernstein, In *Chemistry of Heterocyclic Compounds*, Vol. 11, pp. 718–722; (*b*) F. Liu, K. Wang, G. Bai, Y. Zhang and L. Gao, *Inorg. Chem*, 2004, **43**, 1799–1806.
21 (*a*) G. Stupka, L. Gremaud and A. F. Williams, *Helv. Chim. Acta*, 2005, **88**, 487–495; (*b*) M.-J. Han, L.-H. Gao and K.-Z. Wang, *New J. Chem*, 2006, **30**, 208–214; (*c*) L. Tormo, N. Bustamante, G. Colmenarejo and G. Orellana, *Anal. Chem*, 2010, **82**, 5195–5204.
22 T. Z. Förster, *Electrochem*, 1950, **54**, 42–46.
23 (*a*) M. Albota, J.-L. Beljonne, J. E. Bredas, J.-Y. Ehrlich, A. A. Fu, S. H. Heikal, T. Hess, M. D. Kogej, S. R. Levin, D D. Marder, J. W. McCord-Maughon, H. R. M. Perry, G. Rumi, W. W. Subramaniam, X.-L. Webb and C. Xu, *Science*, 1998, **281**, 1653; (*b*) T. Kohl, K. G. Heinze, R. Kuhlemann, A. Koltermann and P. Schwille, *Proc. Natl. Acad. Sci. USA*, 2002, **99**, 12161.
24 (*a*) J. A. Thomas, R. N. Buchsbaum, A. Zimniak and E. Racker, *Biochem*, 1979, **18**, 2210–2218; (*b*) I. Mellman, R. Fuchs and A. Helenius, *Ann. Rev. Biochem*, 1986, **55**, 663–700; (*c*) N. Nelson, *Curr. Opin. Cell Biol*, 1992, **4**, 654–660.
25 S. Ohkuma and B. Poole, *PNAS*, 1978, **75**, 3327–3331.